MITIGATION OF THE ELECTRON-CLOUD EFFECT IN THE PSR AND SNS PROTON STORAGE RINGS BY TAILORING THE BUNCH PROFILE*

M. Pivi†, SLAC, Menlo Park 94025, California, USA
M. A. Furman, LBNL, Berkeley 94720, California, USA

Abstract

For the storage ring of the Spallation Neutron Source (SNS) at Oak Ridge, and for the Proton Storage Ring (PSR) at Los Alamos, both with intense and very long bunches, the electron cloud develops primarily by the mechanism of trailing-edge multipacting. We show, by means of simulations for the PSR, how the resonant nature of this mechanism may be effectively broken by tailoring the longitudinal bunch profile at fixed bunch charge, resulting in a significant decrease in the electron-cloud effect. We briefly discuss the experimental difficulties expected in the implementation of this cure.

INTRODUCTION

It is becoming progressively clear that the electron-cloud effect plays an important role in the high-intensity instability which has been observed in the PSR at the Los Alamos National Laboratory (LANL) for more than 13 years. This instability is now believed to be due to the collective coupling between an electron cloud and the proton beam [1]. Such instability is a particular manifestation of the electron-cloud effect (ECE) that has been observed or is expected at various other machines. In this article we present simulation results for the SNS ring obtained with the ECE code that has been developed at LBNL, and lately in collaboration with SLAC, over the past 7 years. Besides other possible mitigation effects including Landau damping, TiN coating, clearing electrodes, solenoid windings and electron conditioning [2], we investigate the possibility to suppress the electron formation by tailoring the longitudinal beam profile.

PHYSICAL MODEL

Sources of Electrons

The electron production may be classified into: (1) electrons produced at the injection region stripping foil (2) electrons produced by proton losses incident on the vacuum chamber at grazing angles (3) secondary electron emission process and (4) electrons produced by residual gas ionization. The two main sources of electrons considered for proton storage rings at the SNS and the PSR, are lost protons hitting the vacuum chamber walls, and secondary emission from electrons hitting the walls.

* Work supported by the US DOE under contracts DE-AC03-76SF00515 and DE-AC03-76SF00098.

† mpivi@slac.stanford.edu

Table 1: Simulation parameters for the PSR and SNS.

Parameter	Symbol,unit	PSR	SNS
Ring parameters			
Proton beam energy	E, GeV	1.735	1.9
Dipole field	B, T	1.2	0.78
Bunch population	N_p, $\times 10^{13}$	5	20.5
Ring circumference	C, m	90	248
Revolution period	T, ns	350	945
Bunch length	τ_b, ns	254	700
Gauss. tr. beam size	σ_x, σ_y, mm	10, 10	
Flat tr. beam size	r_x, r_y, mm		28, 28
Beam pipe semi-axes	a, b, cm	5, 5	10, 10
Simulation parameters			
Proton loss rate	p_{loss}, $\times 10^{-6}$	4	1.1
Proton-electron yield	Y	100	100
No. kicks/bunch	N_k	1001	10001
No. steps during gap	N_g	400	1000
Max sec. yield	δ_{max}	2.0	2.0
Energy at yield max	E_{max}, eV	300	250
Yield low energy el.	$\delta(0)$	0.5	0.5
Rediffused component	$P_{1,r}(\infty)$	0.74	0.2

Secondary Emission Process

When a primary electron impinges on the beam pipe surface generates secondary electrons. The main secondary electron yield (SEY) parameters are the energy E_{max} at which $\delta(E_0)$ is maximum, and the peak value itself, $\delta_{\text{max}} = \delta(E_{\text{max}})$, see Table 1 and Fig. 1. For the results shown below, we do take into account the elastic backscattered and rediffused components of the secondary emitted-electron energy spectrum $d\delta/dE$.

Simulation Model

The SNS proton storage ring stores a single proton bunch of length τ_b followed by a gap of length τ_g with a typical current intensity profile shown in Figs. 3 and 5. The transverse beam distribution for the SNS is assumed to be constant with r_x=r_y=28 mm. The vacuum chamber is assumed to be a cylindrical perfectly-conducting pipe. The number of electrons generated by lost protons hitting the vacuum chamber wall is $N_p \times Y \times p_{\text{loss}}$ per turn for the whole ring, where Y is the effective electron yield per lost proton, and p_{loss} is the proton loss rate per turn for the whole ring per beam proton. The lost-proton time distribution is proportional to the instantaneous bunch intensity. The electrons are then simulated by macroparticles. The secondary electron mechanism adds to these a variable number

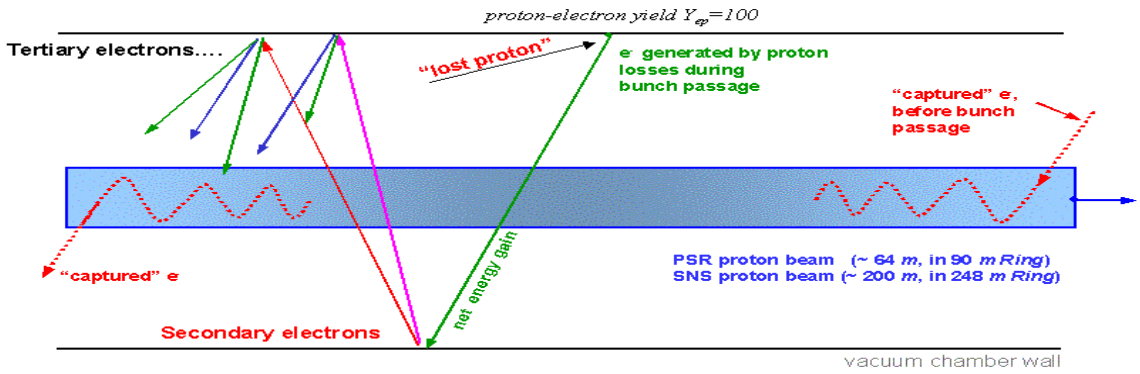

Figure 2: Electron multiplication mechanism in long proton bunches.

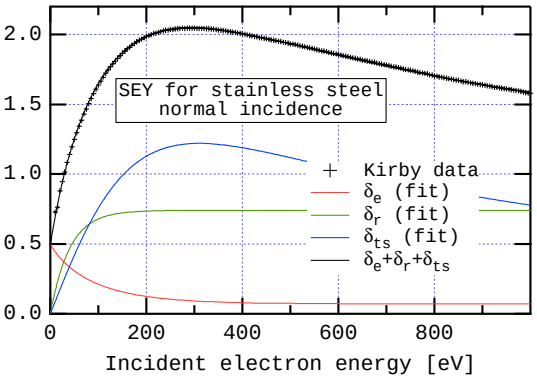

Figure 1: (Color) The SEY for stainless steel for a SLAC standard 304 rolled sheet, chemically etched and passivated but not conditioned (data courtesy R. Kirby.

of macroparticles, generated according to the SEY model mentioned above. The bunch is divided up into N_k kicks, and the interbunch gap into N_g intermediate steps. The image and space charge forces are computed and applied at each slice in the bunch and each step in the gap.

RESULTS AND DISCUSSIONS

An electron present in the vacuum chamber before the bunch passage oscillates in the beam well potential. The oscillation amplitude most likely remains smaller than the chamber radius during the beam passage and the electron is released at the end of the beam passage. On the other hand, electrons generated at the wall by proton losses near the peak of the beam pulse are accelerated and decelerated by the beam potential and hit the opposite wall with a net energy gain, producing secondary electrons, see Fig. 2. Electrons which survive the gap between two bunch passages will increase in number. The electrons gradually increase in number during successive bunch passages until, owing to the space-charge forces, a balance is reached between emitted and absorbed electrons. See also an animation of the PSR electron cloud dynamic during the beam passage at [4].

The estimated build-up of the electron cloud in a PSR field free region gives $\sim$75 nC/m or 6×10^7 e/cm^3 [1].

The SNS beam pipe chamber will be coated with TiN. Recent measurements of an as-received sample of the TiN coated stainless steel SNS vacuum chamber, has shown a secondary electron yield $\delta_{\max} = 1.9 \pm 0.2$ [5, 6].

Due to the large electron multiplication, we have used a relatively small number of macroparticles generated per bunch passage, which leads, nevertheless, to reasonably stable results in terms of the turn-by-turn electron density. The amplification factor per macroparticle may exceed 10^4 during a single bunch passage when $\delta_{\max} = 2$. Simulation results for the SNS obtained with a different code [7] show a qualitative agreement with our results, although they yield a lower estimated electron density at this SEY value [5]. We assume in these simulations that proton losses corresponding to 1.1×10^{-6} protons loss per proton per turn are expected in the SNS ring. The build-up of the electron cloud results in an average line density of 100 nC/m with a line density within the beam radius region exceeding 10 nC/m. These imply neutralization factors as shown in Fig. 3. In particular the neutralization factor dur-

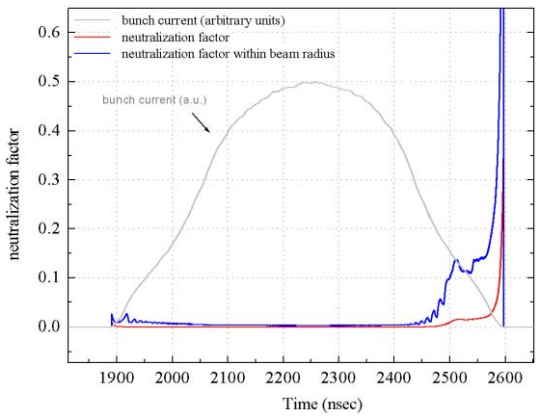

Figure 3: Simulated electron neutralization factor in a SNS field-free region. The fractional charge neutralization computed within the beam radius region is $\sim$ 1% during the bunch passage, and it exceeds 10% at the tail of the bunch.

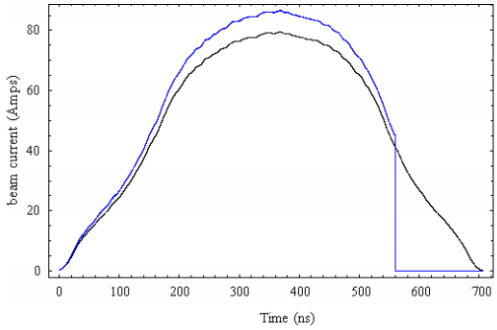

Figure 4: SNS beam current profile cut at 560 ns, compared to the nominal beam profile.

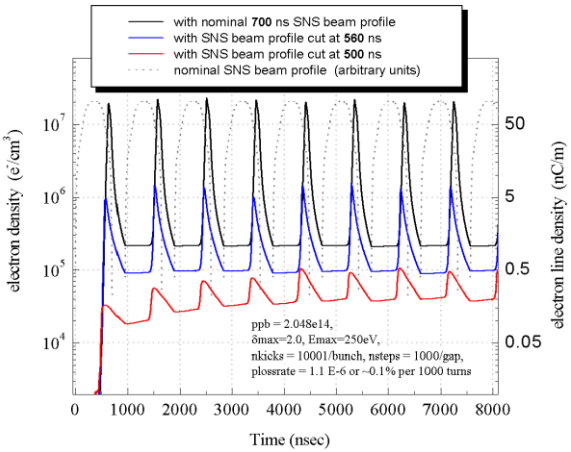

Figure 5: Simulated electron density in an SNS field-free region, assuming $\delta_{\max} = 2$ and $N_p = 2.05 \times 10^{14}$. We have artificially truncated the tail of the bunch, while maintaining the same integrated beam charge. The density of the electron cloud decreases as the tail of the beam is progressively reduced.

ing the bunch passage is 1%, and most of the electrons are contained in the beam radius region.

The possible amplification mechanism which may take place in long-beam storage rings suggest interesting considerations. Electrons generated at the wall by proton losses near the peak of the beam pulse are accelerated and decelerated by the beam potential and hit the opposite wall with a net energy gain, producing secondary electrons. Many generations of secondary electrons may occur during a single bunch passage leading to an high electron cloud density owing to trailing-edge multipacting. In order to verify this assumption, in the simulations, we have artificially truncated the tail of the bunch, while maintaining the same integrated beam charge. In particular, Fig. 4 shows the modified SNS beam current profile, compared to the nominal beam current profile. The effect of the modification of the beam profile on the formation of the electron cloud is shown in the lowest curves of Fig. 5. The density of the electron cloud decreases as the tail of the beam is progressively truncated. Tailoring the 700ns long beam at 560ns and 500ns reduces the peak electron density by a factor 20 and 200 respectively. A reduction of the beam head profile has the opposite effect of increasing the electron cloud density. Simulation results for the PSR have shown a similar behavior.

CONCLUSIONS

We have presented electron cloud simulations for the SNS. When considering proton losses of 10^{-6} and $\delta_{\max}$ =2, a line density of $\geq$ 100 nC/m should be expected in an SNS field-free region, with a density exceeding 10 nC/m within the beam radius region. Although the neutralization factor may exceed 10% near the tail of the beam, the resulting electron cloud tune shift is moderate. Linear stability studies and current threshold estimates are deferred to a separate publication [5]. Many generations of secondary electrons may occur during a long bunch passage leading to an high electron cloud density owing to trailing-edge multipacting. In order to verify this assumption, in the simulations, we have artificially truncated the tail of the bunch, while maintaining the same integrated beam charge.

The density of the electron cloud decreases, more than to 2 orders of magnitude, as the tail of the beam is progressively truncated. Although tailoring the beam is difficult to achieve in practice as alternative method to suppress the formation of the electron cloud, it has been considered as a possible experiment at the PSR. More investigations are needed.

ACKNOWLEDGMENTS

We are indebted to M. Blaskiewicz, K. Harkay, R. Davidson, H. Qin, P. Channell, T. S. Wang for many stimulating discussions. We are especially grateful to R. Macek for kindly providing us the experimental data and for many valuable discussions. Thanks to R. Kirby, A. Alexandrov, V. Danilov. We are grateful to NERSC for supercomputer support.

REFERENCES

[1] Various contributions http://slap.cern.ch/collective/ecloud02/, especially the surveys by M. Blaskiewicz and R. Macek.

[2] J. Wei et al., these proceedings (WPPG004).

[3] For an updated on the self consistent treatment of the instability see Physical Review Special Topic, http://prst-ab.aps.org/Two-Stream Special Collection Edition.

[4] Movie of the electron-cloud in the PSR by M. Pivi at http://slap.cern.ch/collective/ecloud02/newschedule.html

[5] M. Blaskiewicz et al. Phys. Rev. ST Accel. Beams **6**, 014203 (2003).

[6] T. Toyama, K. Ohmi, in *Proceedings of the ECLOUD-02 workshop*.

[7] M. Blaskiewicz , in *Proceedings of the ECLOUD-02 workshop*.